Bioorganic & Medicinal Chemistry Letters 18 (2008) 6151–6155

Contents lists available at ScienceDirect

Bioorganic & Medicinal Chemistry Letters

journal homepage: www.elsevier.com/locate/bmcl

Synthesis and structure–activity relationships of selective norepinephrine reuptake inhibitors (sNRI) with improved pharmaceutical characteristics

Joseph Pontillo [a], Dongpei Wu [a], Brett Ching [a], Sarah Hudson [a], Marc J. Genicot [a], Yinghong Gao [b], Todd Ewing [b], Beth A. Fleck [c], Kathleen Gogas [d], Anna Aparicio [e], Hua Wang [e], Jenny Wen [e], Warren S. Wade [a,*]

[a] Department of Medicinal Chemistry, Neurocrine Biosciences, Inc., 12790 El Camino Real, San Diego, CA 92130, USA
[b] Department of Computational Chemistry, Neurocrine Biosciences, Inc., 12790 El Camino Real, San Diego, CA 92130, USA
[c] Department of Pharmacology, Neurocrine Biosciences, Inc., 12790 El Camino Real, San Diego, CA 92130, USA
[d] Department of Neuroscience, Neurocrine Biosciences, Inc., 12790 El Camino Real, San Diego, CA 92130, USA
[e] Department of Preclinical Development, Neurocrine Biosciences, Inc., 12790 El Camino Real, San Diego, CA 92130, USA

ARTICLE INFO

Article history:
Received 14 August 2008
Revised 30 September 2008
Accepted 2 October 2008
Available online 7 October 2008

Keywords:
Norepinephrine
Serotonin

ABSTRACT

The design synthesis and SAR of a series of chiral ring-constrained norepinephrine reuptake inhibitors with improved physicochemical properties is described. Typical compounds are potent (IC_{50}s <10 nM), selective against the other monoamine transporters, weak CYP2D6 inhibitors (IC_{50}s > 1 μM) and stable to oxidation by human liver microsomes. In addition, the compounds exhibit a favorable polarity profile.

Monoamine reuptake inhibition has been an effective therapeutic intervention in a variety of CNS diseases starting with depression, and recently expanding to include chronic pain, ADHD, and stress urinary incontinence.[1–4] We were interested in multiple indications in the therapeutic spectrum of sNRI compounds and initiated work directed toward finding potent and selective compounds with good pharmaceutical properties and minimal risk of drug–drug interactions.[5–7] In the previous letter,[7] a series of chiral sNRIs with improved stability was reported. However, the overall hydrophobicity of the best compounds severely limited the ability to avoid CYP2D6-related drug–drug interactions with marketed pharmacotherapies. Further work directed at providing a larger range of potential drug candidates is reported here.

Compounds in the previously discovered series, shown in Figure 1, were generally more hydrophobic than atomoxetine, and unfortunately, hydrophobicity correlated with greater CYP2D6 inhibition. Substitution on the aryloxy ring resulted in large changes in NET/SERT selectivity, and therefore was limited in scope. Consequently, it was necessary to look for modifications of the core structure that maintained potency at NET while being intrinsically more hydrophilic. In addition, synthesis of the more potent cis diastereomers like **3** and **4** was difficult, especially for electron-rich aromatic rings that gave the best potency and selectivity. If possible, a series where synthesis of the *cis* diastereomer was straightforward, even for electron-rich aryl groups, and with no additional stereocenters would be preferred. These requirements were met with the hydroxyindane core shown in Scheme 1.

Synthesis of the hydroxyindane compounds proceeded from the known hydroxymethylindene **5**.[8] Following protection as the TBS ether, epoxidation was performed with *m*CPBA, and the resulting epoxide **6** was subsequently opened with the anion of a phenol or thiophenol, illustrated in Scheme 1 for the direct analogs of atomoxetine. During the epoxide opening, concomitant partial to full deprotection occurred. In the cases of partial deprotection, tetrabutylammonium fluoride was added to the crude mixtures to generate diol **7** in good yields. Installation of the amine followed a three step procedure that was best accomplished in one pot. Formation of the primary mesylate was followed by conversion to the *exo* epoxide that was then opened with a primary or secondary amine to give predominantly the aminomethyl regioisomer. For the carbon analog, epoxide **6** was opened with an in situ generated cuprate, and the resultant diol **10** was converted to the amine under similar conditions. This sequence ensured the relative stereochemistry observed for previous compounds,[7] where the aryloxy group and aminomethylene groups are *cis* relative to each other. A crystal structure of **26-II**,[9] the inactive enantiomer of **26-I** in Table 2, established that the two oxygen substituents are in the

* Corresponding author. Tel.: +1 858 617 7600; fax: +1 858 617 7601.
E-mail addresses: shudson@neurocrine.com (S. Hudson), warrenswade@gmail.com (W.S. Wade).
URL: http://www.neurocrine.com (W.S. Wade).

0960-894X/$ - see front matter © 2008 Elsevier Ltd. All rights reserved.
doi:10.1016/j.bmcl.2008.10.013

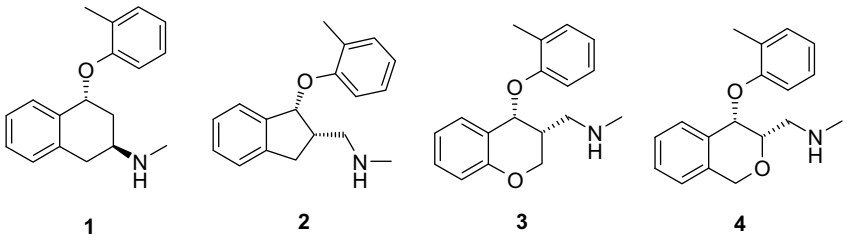

Figure 1. Structures of the active enantiomers of four ring-constrained isomers of atomoxetine reported previously.[5–7]

pseudoaxial position, as had been observed previously for the aryloxy ring.[7] The less active enantiomer was produced in reasonable quantity during the chiral separation of **26-I** for in vivo studies. The hydroxyl anion of Boc-protected **8-I** could be alkyated with methyl iodide then deprotected under acidic conditions to generate **12-I**.

Two variants of this sequence were performed, as shown in Scheme 2. For the primary amine products (e.g., **16**), azide anion was used as the nucleophile to give **15** that was then reduced using a Staudinger reduction.[10] The alternative diastereomer could most easily be synthesized starting with diol **7** and reversing the direction of formation of the *exo* epoxide. After protection of the primary alcohol as the TBS ether and formation of the tertiary mesylate **17**, deprotection of the primary alcohol, anionic epoxide formation and ring opening with methylamine generated **18**. The intermediates in this sequence were sensitive to elimination. Consequentially, yields were considerably lower.

The synthesis of compounds **21** and **23** is shown in scheme 3. A tandem alkylation/aldol reaction generated **19** as the major diastereomer that could be selectively crystallized from hexane/ethyl acetate. Aryl substitution proceeded normally to generate both diastereomers of the methyl dihydrofuran core. The relative stereochemistry of **23** was established by NOE.

Compound enantiomers were initially separated by chiral HPLC, but it was found that chiral **7** could be produced in high optical purity (85–90%ee) under Jacobsen epoxidation conditions.[11] Recrystallization of the final product salts then gave material with 95–99%ee. Compound **24** proved difficult to separate via chiral HPLC, so synthesis of **24-I** was accomplished by the chiral route. The more active enantiomer consistently showed a positive optical

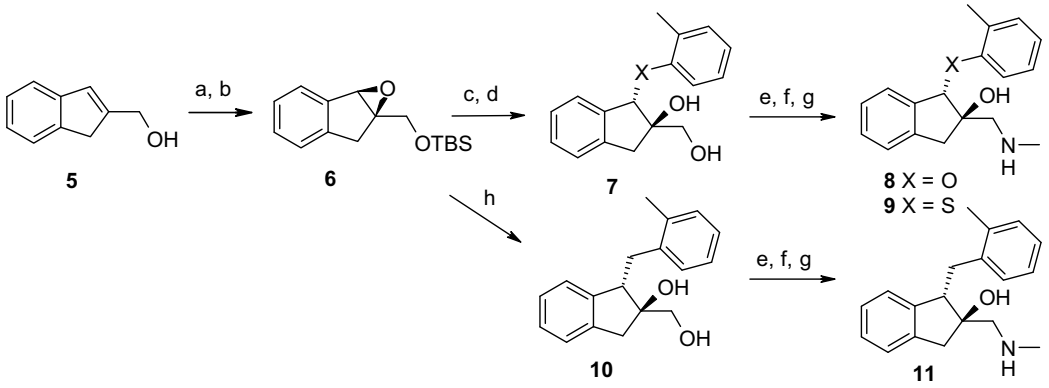

Scheme 1. Reagents and conditions: (a) TBSCl, TEA, DMAP, DCM, rt, 3 h, 90%; (b) *m*CPBA, $NaHCO_3$, DCM, 0 °C, 6 h; (c) ArylXH, NaH, DMSO, then **6**, 75 °C, 18 h; (d) TBAF, THF, rt, 10 min, 60–70% for combined steps (b–d); (e) Ms_2O, TEA, DCM, −30 to 0 °C, 1 h; (f) K_2CO_3, DMF, rt, 1.5 h; (g) methylamine, THF, 70 °C, 18 h, 30–70% for three steps; (h) 2-MeBnMgBr, CuI, THF, −78 °C, 0.25 h, then **6**, −40 to −20 °C, 3 h, 74%.

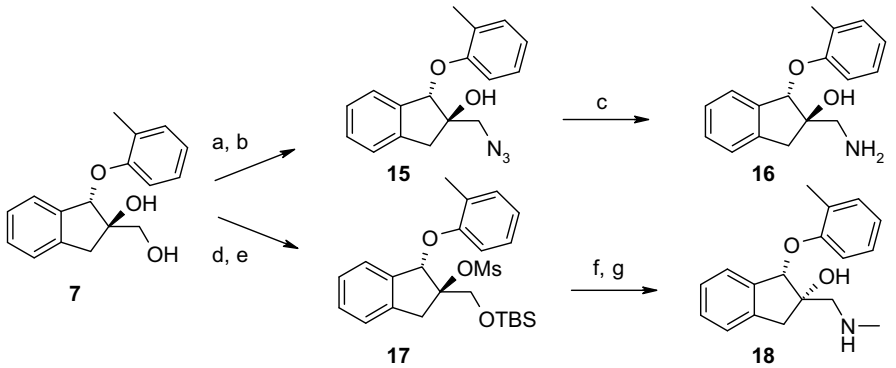

Scheme 2. Reagents and conditions: (a) MsCl, TEA, DCM, 0 °C, 1 h; (b) K_2CO_3, DMF, rt, 2 h, then NaN_3, 15-*crown*-5, 70 °C, 18 h, 75% for two steps; (c) PPh_3, THF, rt, 1 h then H_2O, 65 °C, 1 h, 78%; (d) TBSCl, TEA, DCM, 0 °C–rt, 16 h, 50%; (e) MsCl, TEA, DCM, 0 °C–rt, 18 h, 21%; (f) TBAF, THF, rt, 1 h, 63%; (g) NaH, DMA, rt, 1.5 h, then methylamine, 55 °C, 18 h, 7%.

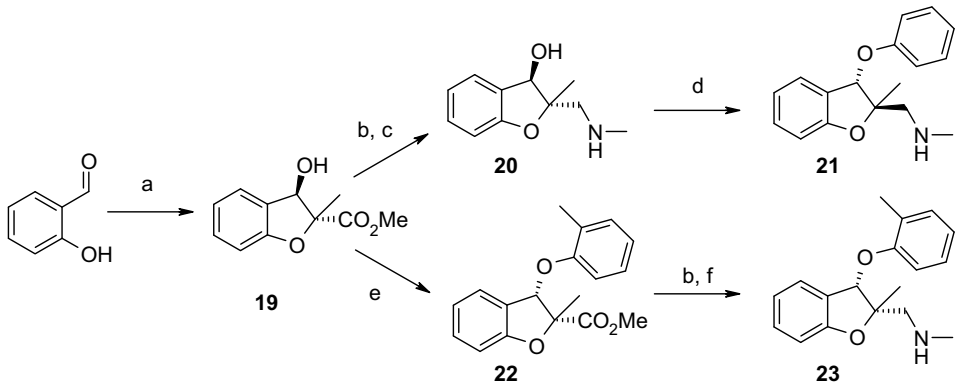

Scheme 3. Reagents and conditions: (a) Methyl 2-bromopropionate, K_2CO_3, DMF, 100 °C, 16 h, 60%; (b) DiBAlH, DCM, −78 °C, 2 h; (c) Methylamine, BH_3.pyr, THF, rt, 16 h, 10% (two steps); (d) 2-Fluorotoluene, NaH, DMSO, 80 °C, 16 h, 10%; (e) 2-Methylphenol, PPh_3, DEAD, THF, rt, 18 h, 32%; (f) Methylamine, $Na(OAc)_3BH$, THF, rt, 16 h, 50% (two steps).

rotation. Absolute conformations were determined by analogy to the aforementioned crystal structure of **26-II**.

All compounds were tested for their ability to inhibit norepinephrine, serotonin and dopamine uptake in HEK cell lines that had been stably transfected with the human transporters. Compounds were initially tested in two independent dose–response experiments, and those with reasonable potency at NET were retested multiple times. Atomoxetine was included on all assay plates as a standard control, and assay variability was reasonable for a functional assay with SEM values typically below 0.2 log units. Potency values are reported as IC_{50}, though with the neurotransmitter concentrations in each assay well below their respective K_m values, little difference would be expected between the measured IC_{50} and K_i of the compounds. Active compounds were further tested in transporter binding assays by competition with the appropriate radioligand. For all compounds, active functional inhibition at NET (IC_{50}) correlated well with displacement of ^{3}H-nisoxetine from its NET binding site (K_i). All compounds were tested for inhibition of CYP3A4 and CYP2D6 activity,[12] and the metabolic stability in human liver microsomes was also measured for NET active compounds.[13] As expected, no significant inhibition of CYP3A4 was observed for any of these compounds.

Initial testing of the hydroxyindane racemates indicated that the activity observed with **2**–**4** and atomoxetine was retained in the hydroxyindanes. SAR (Table 1) matched that observed for previous series at the amine site,[6] with **8** being the most potent, the primary amine **16** being slightly less active and the ethyl amine **13** 20-fold less potent. In this series, the sulfur and carbon analogs at the ring junction, **9** and **11**, were synthetically accessible and maintained potency at NET. Upon separation of the racemate, the direct analog of atomoxetine in this series, **8-I**, was indistinguishable from atomoxetine in the inhibition of all three transporters and CYP2D6. Consistent with previous series,[7] the absolute configuration of the active enantiomer **8-I** matches atomoxetine and reboxetine.

Positioning and substitution of the hydroxyl group was critical for activity (Fig. 2). The alternative diastereomer, **18**, was >100-fold less active, and both diastereomers of the regioisomeric 2-methylbenzofuran **21** and **23** were completely inactive. Additionally, methylation of **8-I** to generate **12-I** removed all transporter

Table 1
SAR of the hydroxyindane core[a]

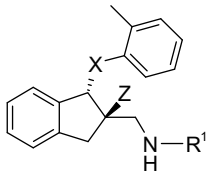

Compound	Isomer	X	Z	R^1	NET[b]	SERT[b]	DAT[b]	CYP2D6[c]	*c*Log *P*[d]
Atomoxetine	R			Me	5	180	3000	2000	3.3
2	*R,S*	O	H	Me	7	1,400	3500	800	3.9
8	rac	O	OH	Me	30	700	2700	2300	3.1
8-I	*S,R*	O	OH	Me	3	184	1600	2000	3.1
8-II	*R,S*	O	OH	Me	770	5500	2300	2500	3.1
9	rac	S	OH	Me	10	1400	4700	400	3.6
11	rac	C	OH	Me	30	2500	>10,000	900	3.7
12-I	*S,R*	O	OMe	Me	>10,000	>10,000	>10,000	5000	3.6
13	rac	O	OH	Et	700	5700	>10,000	1300	3.6
14	rac	O	OH	CH_2CH_2OH	2,800	3500	>10,000	>10,000	2.5
16	rac	O	OH	H	75	4000	>10,000	4000	2.8
16-I	*S,R*	O	OH	H	77	3000	>10,000	3300	2.8

[a] Transporter data are the average of two or more independent measurements.
[b] IC_{50} (nM) for inhibition of monoamine uptake.
[c] IC_{50} (nM) for inhibition of CYP2D6.[12]
[d] Calculated Log *P*.[14]

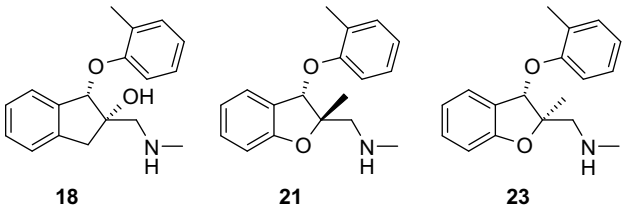

Figure 2. Inactive isomers of **8**.

activity, as did adding an additional hydroxyl group near the amine position (see **14**).

Selectivity against an in-house panel of receptors for amine neurotransmitters (selected dopamine, serotonin, adrenergic, and muscarinic receptors) revealed no activity for these compounds except at the 5HT2b receptor (500 nM–2 μM). This represents >100-fold selectivity against other proteins that interact with the same substrates and is an improvement over the 30-fold selectivity of both **1** and **2** against 5HT2b. Similar selectivity is observed for atomoxetine against this receptor.[14]

CYP2D6 inhibition maintained the trend observed previously,[7] where hydrophobicity contributes to increased inhibition. Compared to **2**, **8-I** was 3-fold less potent at CYP2D6 and the calculated log *P*[15] was about 0.8 log units lower. As the hydrophobicity of the ring attachment atom increased from O to C to S, CYP2D6 activity also increased to IC_{50} values below 1 μM. Unlike previous compounds, there was no significant difference in CYP2D6 inhibition between enantiomers (e.g., **8-I**/**II**).[7]

SAR for aryloxy ring substitution for the active enantiomers is shown in Table 2. Similar activity trends were observed for both methyl and fluoro substitution of **8-I**, with 4-substitution generating compounds nearly equipotent on SERT (**32-I** and **34-I**). Selectivity improved to ⩾12-fold with 3-substitution, and the other isomers were more selective. CYP2D6 inhibition remained in the micromolar range for all fluoro isomers, an improvement over previous series.[7] Halogen substitution at the 2 position (**25-I** and **26-I**) also generated potent and selective compounds with reasonable CYP2D6 activity. In this series as well, 2-methoxy substitution resulted in both a decrease in activity at NET and an increase in activity at CYP2D6. Overall the most potent and selective compound was **27-I**, though the CYP2D6 inhibition of this compound was just below 1 μM. Oxidative clearance in microsomes was significantly lower than atomoxetine for this series, with several compounds exhibiting no measurable loss of parent in a 60-min incubation. The only exceptions were methyl substitution of **8-I** to give compounds **31-I** and **32-I**, where there is the potential for benzylic oxidation and the naphthyl compound, **24-I**.

To further ameliorate the CYP2D6 inhibition, more polar substitution of the aryloxy ring was evaluated. Hydroxyl substitution on the methyl of **8-I** to generate **30-I** was not tolerated. However, as had been observed previously,[7] phenolic substitution at the 4-position generated the potent yet nonselective transporter inhibitor **38-I**. Neither compound displayed significant CYP2D6 inhibition. Like the fluorine substituted compounds, 3-hydroxy substitution (**37-I**) improved the selectivity over SERT to 20-fold and maintained minimal CYP2D6 inhibition. Oxidative clearance remained low for these compounds, though the phase II clearance is unknown. The equivalent metabolite in atomoxetine is converted rapidly to the glucoronide in vivo.[14]

Overall, this series produced a number of potent and selective compounds with advantageous stability and similar or better CYP2D6 inhibition compared with atomoxetine. Accordingly, a number of compounds identified were tested for in vivo activity and the results will be reported in future publications.

Acknowledgments

The authors are indebted to Mr. Brock Brown and Ms. Kathy Barrett for technical support in the transporter assays and Dr. Tao

Table 2
SAR of the aryloxy ring in the hydroxyindanes[a]

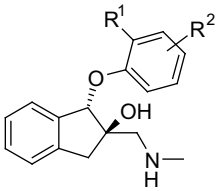

Compound	Isomer	R^1	R^2	NET[b]	SERT[b]	DAT[b]	CYP2D6[c]	Clearance[d]
8-I	*S*,*R*	Me		3	184	1600	2000	10
24-I	*S*,*R*	1-Napthyl		3	10	10,000	600	23
25-I	*S*,*R*	F		11	700	4000	4000	⩽3
26-I	*S*,*R*	Cl		5	700	10,000	2000	10
27-I	*S*,*R*	Et		1.5	800	>10,000	800	⩽3
28-I	*S*,*R*	OMe		17	2200	>10,000	500	⩽3
29-I	*S*,*R*	SMe		2	500	>10,000	1400	43
30-I	*S*,*R*	CH_2OH		300	1800	>10,000	>10,000	ND
31-I	*S*,*R*	Me	3-Me	3	50	3500	4000	43
32-I	*S*,*R*	Me	4-Me	2	5	8000	6500	32
33-I	*S*,*R*	Me	3-F	3	36	3000	1500	⩽3
34-I	*S*,*R*	Me	4-F	5	6	5000	1500	⩽3
35-I	*S*,*R*	Me	5-F	7	200	>10,000	1000	7
36-I	*S*,*R*	Me	6-F	5	150	>10,000	1000	17
37-I	*S*,*R*	Me	3-OH	4	100	4000	>10,000	6
38-I	*S*,*R*	Me	4-OH	4	14	5000	>10,000	10

[a] Transporter data are the average of two or more independent measurements.
[b] IC_{50} (nM) for inhibition of monoamine uptake.
[c] IC_{50} (nM) for inhibition of CYP2D6.[12]
[d] Scaled intrinsic clearance (mL/min/kg) in human liver microsomes,[13] clearance of ⩽3 indicates no detectable compound loss. ND, not done.

Hu and Ms. Mila Lagman for chiral chromatography development and purification.

Supplementary data

Supplementary data associated with this article can be found, in the online version, at doi:10.1016/j.bmcl.2008.10.013.

References and notes

1. Jann, M. W.; Slade, J. H. *Pharmacotherapy* **2007**, *27*, 1571.
2. Babu, R. P. K.; Maiti, S. N. *Heterocycles* **2006**, *69*, 539.
3. Zhou, J. *Drugs Future* **2004**, *29*, 1235.
4. Wernicke, J. F.; Iyengar, S.; Ferrer-Garcia, M. D. *Curr. Drug Ther.* **2007**, *2*, 161.
5. Wu, D.; Pontillo, J.; Ching, B.; Hudson, S.; Gao, Y.; Fleck, B. A.; Gogas, K.; Wade, W. S. *Bioorg. Med. Chem. Lett.* **2008**, *18*, 4224.
6. Hudson, S.; Kiankarimi, M.; Eccles, W.; Mostofi, Y. S.; Genicot, M. J.; Dwight, W.; Fleck, B. A.; Gogas, K.; Wade, W. S. *Bioorg. Med. Chem. Lett.* **2008**, *18*, 4495.
7. Hudson, S.; Kiankarimi, M.; Eccles, W.; Dwight, W.; Mostofi, Y. S.; Genicot, M. J.; Fleck, B. A.; Gogas, K.; Aparicio, A.; Wang, H.; Wen, J.; Wade, W. S. *Bioorg. Med. Chem. Lett.* **2008**, *18*, 4491.
8. Palandoken, H.; McMillen, W. T.; Nantz, M. H. *Org. Prep. Proceed. Int.* **1996**, *28*, 702.
9. Generated at the UCSD Small-Molecule Crystallography Facility. The crystal system and space group assignments were unambiguous, and the absolute stereochemistry was established by Flack parameter refinement. All non-hydrogen atoms were refined anisotropically and hydrogen atoms were placed in idealized locations. All software was contained in the APEX, SAINT, and SHELX software packages distributed by Bruker-AXS, Madison, WI. Crystal data for **26-II**: $C_{15}H_{19}Cl_2NO_2$, monoclinic, $P2_1$, $a = 7.8168(12)$, $b = 5.8834(8)$, $c = 18.473(3)$ Å, $\beta = 102.160(2)^\circ$, $V = 830.5(2)$ Å^3, $Z = 2$, $T = 208$ K. $R(F) = 5.89\%$ based on 2172 independent reflections.
10. Gololobov, Y. G.; Zhmurova, I. N.; Kasukhin, L. F. *Tetrahedron* **1981**, *37*, 437.
11. Hughes, D. L.; Smith, G. B.; Liu, J.; Dezeny, G. C.; Senanayake, C. H.; Larsen, R. D.; Verhoeven, T. R.; Reider, P. J. J. *Org. Chem.* **1997**, *62*, 2222.
12. Recombinant CYP2D6 or CYP3A4 was incubated with a marker substrate and a NADPH-generating system for 30 min at 37 °C in the presence of varying concentrations of test compound. CYP3A4 activity was quantitated from the cleavage of substrate BFC to its fluorescent product 7-HFC. Ketoconazole was used as a positive control. CYP2D6 activity was quantitated from the cleavage of AMMC to its fluorescent product AHMC. Quinidine was used as positive control.
13. Test compounds were incubated at 1 μM concentration in the presence of pooled human liver microsomes (0.5 mg/mL; $n > 10$; mixed gender) in the presence of an NADPH-generating system. The rate of disappearance of the parent compound was quantitated by LC/MS/MS at five time points over 60 min and the measured rate scaled to human body mass.
14. Sauer, J.-M.; Ring, B. J.; Witcher, J. W. *Clin. Pharmacokinet.* **2005**, *44*, 571.
15. Calculated log*P*s were determined using ACD/LogP DB, version 9.02, Advanced Chemistry Development, Inc., Toronto, ON, Canada, http://www.acdlabs.com, 2005. Calculated and measured values for atomoxetine, **8-I**, and **16-I** were the same within experimental error.